Available online at www.sciencedirect.com
SCIENCE DIRECT®
ELSEVIER
International Journal of Mechanical Sciences 45 (2003) 1449–1465
International Journal of MECHANICAL SCIENCES
www.elsevier.com/locate/ijmecsci

# Micromechanical modeling of dual phase steels

F.M. Al-Abbasi, J.A. Nemes*

*Department of Mechanical Engineering, McGill University, 817 Sherbrooke Street West, Montreal, Que., Canada H3A 2K6*

Received 12 February 2003; received in revised form 22 October 2003; accepted 5 November 2003

**Abstract**

Dual phase (DP) steels having a microstructure consisting of a Ferrite matrix, in which particles of Martensite are dispersed, have received a great deal of attention due to their useful combination of high strength, high work hardening rate and ductility, all of which are favorable properties for forming processes. Experimental investigation into the effect of the harder phase volume fraction, morphology and phase distribution on mechanical properties of the dual phase steels is well established and comprehensive in the literature. In the present work, a micromechanical model is developed to capture the mechanical behavior of such materials, adopting the constitutive behavior of the constituents from the literature. Analytical approaches have been used in the past to model the DP steel material behavior, but theoretical treatments are based on the assumption of uniform deformation throughout the constituents, neglecting the local strain gradients. This assumption contradicts experimental observations, reduces the understanding of the mechanics and mechanism of deformation of such materials. Based on the micromechanical modeling of cells, several idealizations are investigated out of which the axisymmetric model is shown to display intrinsic ability to capture the expected material behavior in terms of the trend of the stress–strain curves with increasing volume fraction of the second phase and in terms of the deformation fields of the constituents.


*Keywords:* Dual phase; Constitutive; Elastic–plastic; Homogenization; Microstructural; Micromechanical and steel

## 1. Introduction

It is well established that low-carbon multiphase (MP) steels developed in the past decades offer impressive mechanical properties, such as high work hardening rate and good ductility, which also have the advantage of reduced cost, superior formability, and excellent surface finish over other

* Corresponding author. Tel.: +1-514-398-6289; fax: +1-514-398-7365.
*E-mail address:* james.nemes@mcgill.ca (J.A. Nemes).

0020-7403/$ - see front matter © 2003 Elsevier Ltd. All rights reserved.
doi:10.1016/j.ijmecsci.2003.10.007

high-strength low-alloy (HSLA) steels. Experimental investigation into the effect of size, morphology and phase distribution of MP steels has been comprehensively reported in the literature with focus on having two phases. The advantages of dual phase (DP) steels were first reported by Rashid [1]. The pearlitic HSLA steels developed by microalloying with different additives have shown significant increase in strength compared to the commercial plain carbon steels, but are inferior in terms of ductility and formability. Rashid and Cprek [2] reported results of annealed vanadium alloyed steel (GM 980X) to display a promising decrease in the yield strength, higher ultimate strength, higher work hardening rate, and elimination of yield point elongation with considerable increase in ductility and formability.

Tremendous efforts since the above report was released have been placed on exploring various aspects of DP steels. The effect of volume fraction ($V_m$) of the harder phase (Martensite) has been investigated by different authors (Jiang et al. [3], Bag et al. [4], Tomita [5], Byun and Kim [6] and Tomota [7]). Increasing the volume fraction of the harder phase was found to increase the yield and ultimate strengths of the aggregate. Bag et al. [4] reported that the increase in strength with $V_m$ only extends up to $V_m \sim 55\%$, after which a reduction in strength is observed. The same was observed by Byun and Kim [6] but at a different value of $V_m$. Shen et al. [8] have observed this as well without specifying the value of $V_m$ at which this takes place. They attribute this to carbon dilution, which softens the Martensite phase, thus dropping the overall strength of the aggregate. This can also be elucidated by considering the Joaul–Crussard analysis reported by Byun and Kim [6] where they show that the stages of strain hardening display three distinct regions for $V_m$ less than 30% and two stages of strain hardening for $V_m$ greater than 30%.

Shen et al. [8] have shown, using a scanning electron microscope equipped with a tensile straining stage, that the distribution of the strains between the Ferrite and Martensite phases, as well as among the different grains of each phase was observed to be inhomogeneous. They observed that the Ferrite phase deformed immediately and at a much more rapid rate than the delayed deformation of the Martensite. They have also shown, using scanning electron microscopy, that at low $V_m$ only the Ferrite matrix deforms, with no measurable strain occurring in the Martensite particles. At high $V_m$, however, they have shown that shearing of the interface between the Martensite and Ferrite occurs extending the strain into the Martensite islands after the Ferrite matrix is excessively strained, which is in agreement with Rashid and Cprek [2]. They add, that when the %C is constant as $V_m$ increases, the difference in the strain in the two phases decreases, in agreement with above observations mentioned in the last paragraph. Observations by Rashid and Cprek [2] also indicate that the Martensite phase deforms after excessive straining of the Ferrite matrix due to load being transferred to Martensite islands through the Martensite–Ferrite interface. This is in contrast to other HSLA steels, where the Ferrite phase deforms while the harder phase does not experience any significant deformation. The strain distribution between the phases in the DP steels is believed to delay necking and strain to fracture as indicated by a higher strain rate index compared to the other HSLA steels.

The different stages of strain hardening have been attributed [2,4,6,7] to the following phases of deformation:

(1) Both component phases are elastic.
(2) The softer phase is deformed plastically while the harder phase only elastically.
(3) Both components deform plastically.

Micromechanical modeling of DP steels has received little attention, despite their attractive combination of high strength and toughness. Questions regarding optimum phase combinations persist and accurate predictive models are necessary to minimize costly trial-and-error methods of development. Micromechanical models are used to understand the local mechanics and mechanisms governing the macroscopic elastic–plastic deformation of heterogeneous solids. They provide overall behavior from known properties of the individual constituents and their detailed interaction unlike the macromechanical approach where the heterogeneous structure behavior has to be known to predict the aggregate behavior using a computational model.

Many early works in micromechanical modeling focused on voids within a solid matrix. McClintock [9] considered the evolution of a single cylindrical void in an infinite matrix subjected to axisymmetric loading at the remote boundary. Rice and Tracy [10] used a variational approach to investigate the response of an isolated spherical void in an infinite medium. Both authors considered a rigid perfectly plastic material. Numerous authors have proposed improvement to these works. Gurson [11] proposed approximate yield criteria for ductile porous media using a micromechanical approach. Tvergaard [12] used Gurson's yield criteria and introduced the micromechanical modeling of cells based on a random distribution of particles that can be idealized by considering a regular three-dimensional array of hexagonal cylinders of a matrix material, each containing a spherical void or particle. The problem was further simplified by modeling axisymmetric geometry, where Tvergaard assumed that an infinite series of stacked circular cylinders containing spherical particles is a good approximation for the three-dimensional stacked hexagonal array. Symmetry arguments are then used to limit the RVE to 1/4 of the axisymmetric cell.

Since Tvergaard introduced his stacked hexagonal array (SHA) model, different investigators have used it to model materials of widely different groups. Numerous investigators have shown through experimental and modeling studies that the distribution of the phases strongly affects the macroscopic material response due to the different deformation fields and localization, which arises in the matrix. A comprehensive review of this work is given by Socrate and Boyce [13]. Hung and Kinloch [14] modeled toughening mechanisms of rubber-modified epoxy polymers using both axisymmetric and plane strain RVEs. The plane strain staggered square array model was reported to better capture the prevailing direction of shear distribution which appears to be at an angle of approximately $\pm 45^\circ$ to the direction of the applied load. This pattern was captured for different materials by many authors as reported in Socrate and Boyce [13]. However, Socrate and Boyce reported that while unit cell RVEs based on the staggered square array can effectively capture some important features of the deformation patterns, they cannot truly represent the complexity of the two-phase material and may misrepresent the effect of the actual three-dimensional nature of the structure. Socrate and Boyce [13] studied the micromechanics of toughened polycarbonate and compared the traditional SHA model to the V-BCC model they developed which differs from the SHA model only in the boundary condition at one side of the model. They reported that at high volume fractions of the second phase, the V-BCC model accurately captures the trend of the stress–strain curves while the SHA model does not. In a more recent paper, Socrate et al. [15] modeled multiple crazing in high-impact polystyrene using the SHA model. Tzika et al. [16] studied micromechanics of deformation in particle toughened polyamides, where they used the SA RVE with boundary conditions similar to that in Tvergaard [17] in a study of cavity growth and interaction between small and large voids. Neither the SHA model nor the V-BCC model developed by Socrate and Boyce were similar to the material phenomenon and consequently the SA model was used.

Of particular relevance to the class of materials examined in this study is the work by Ishikawa et al. [18], where the authors have developed a micromechanical model for Ferrite–Pearlite DP steel. They used the SHA and the V-BCC models and reported that the V-BCC model could better capture the general stress–strain trend in terms of the strain hardening. Huper et al. [19] have also developed a micromechanical model for the Ferrite–Bainite DP steel using the plane strain idealization and reported stress–strain curves based on assumed single-phase material behavior.

In this work, a micromechanical model for the Ferrite–Martensite steel is developed. Neither of these phases will undergo transformation as a result of deformation at room temperature, which is the condition being addressed. The importance of this type of steel prevails in its appealing combination of strength and ductility compared to other DP steels modeled in earlier work. Martensite volume fractions as high as 59% are considered. Different idealizations based on the micromechanical modeling of cells are explored and compared. The examination of the idealized models is carried out from two perspectives in parallel. Rather than looking only at the general stress–strain trend as presented in previous studies, the deformation fields of the constituents are examined and compared to the experimental results of Shen et al. [8] and Rashid and Cprek [2], as a means of assessing which idealization better describes the real material behavior. In addition, by considering aggregate strains up to 35%, the model's ability to capture the gain in strength and uniform strain as the $V_m$ increases to a certain level and then a reduction of uniform strain and gain of strength as the $V_m$ is further increased, is also investigated. This tradeoff between strength and uniform strain is an extremely important factor in the optimization of microstructures for DP steels. Moreover, accurate prediction of strain distribution between phases and within each phase is equally important, particularly when related to the development of theories to describe ductile failure or failure under fatigue loading.

## 2. Micromechanical modeling

The unique mechanical properties of the MP steels are attributable to their microstructure, which can be considered on several levels, all of which influence the final behavior of the material. At the finest, is the structure of individual atoms in space, which influence the electrical, magnetic, thermal and elastic behavior of the material. At the next level, is the arrangement of atoms in space at which most metals retain a regular atomic arrangement or crystal structure. The crystal structure in each phase influences the mechanical properties of metals such as ductility and strength. Dislocations, imperfections happening in nature, exist and may be controlled to produce profound changes in properties. At the third level, is the grain structure; the crystal structure changes its orientation between grains, thus influencing material properties. Finally, in many materials, more than one phase is present with each phase having its unique crystal structure and properties. Control of the type, size, distribution, and amount of each phase within the main body of the material provides additional ways to control properties.

It is reasonably easier and cheaper to model on the fourth level as each constituent of the material (each phase) can be considered a homogeneous isotropic part of the aggregate while from the atomic to the grain levels of structure, the properties are not realistically represented by an isotropic continuum. In addition, in modeling the material to capture its essential behavior requires a certain size of volume element, which embodies the essential features of the microstructure, and this is

not feasible on the finer levels but, reasonably, possible on the phase structure level. Furthermore, controlling the microstructure on the finer levels requires addition of costly alloying elements, in addition to the heat treatment processes required, unlike controlling the phase size, shape, volume fraction and distribution which can be achieved by controlling the heat treatment processes alone. Finally, considering the microstructure on this level will enhance unique properties already developed by alloying and is considered as the ultimate in material processing, that can be achieved at low cost.

Micromechanical analysis of MP materials provides overall (aggregate) behavior from known properties of the individual constituents and their detailed interaction. On the other hand, in the macromechanical approach, the heterogeneous structure behavior has to be known to predict the aggregate behavior using a computational model. Another advantage in modeling micromechanically is that all phase combinations of different size, morphology, phase distribution and volume fraction can be analyzed by only having the constituent's mechanical behavior.

Micromechanical models are frequently invoked in order to understand the local mechanics and mechanisms governing the macroscopic elastic–plastic deformation of heterogeneous solids. There are three basic features to a micromechanical model for a generic MP composite:

(a) Geometric definition of a representative volume element (RVE), which embodies the essential features of the microstructure.
(b) The constitutive description of the mechanical behavior of each phase and the interface boundaries, whenever applicable.
(c) A homogenization strategy (procedure) for macroscopic mechanical behavior of the aggregate based on the response of the RVE [13].

### 2.1. Representative volume element (RVE)

A prominent feature of the micromechanical modeling of cells is the transition from a medium with a periodic microstructure to an equivalent homogeneous continuum, which effectively represents the composite material. In a two-phase microstructure, a spatially periodic RVE is assumed to deform in a repetitive way and each RVE resembles its neighboring cells in all aspects. This is indeed a simplifying assumption, but has proved to be satisfactory and is widely accepted. The extent to which the RVE captures the behavior of the microstructure depends in a way on how accurately the RVE captures the morphological features of the actual microstructure [13].

Modeling the microstructure based on plane strain or axisymmetric cell models reduces the complexity of 3D modeling and minimizes the computational cost. Different idealizations based on plane strain or axisymmetric models are reported in the literature, all of which proved to capture the essential real material behavior to some degree. Huang and Kinloch [14] concluded after comparing results of 3D models with previous work, that axisymmetric models could be used without significant loss in accuracy.

The simplest plane strain idealization that is used to represent the periodic array of a two-phase material is based on a simple square array (PS1) with axes of the array parallel to the loading direction, as shown in Fig. 1a. As an alternative, the staggered square array (PS2), shown in Fig. 1b, eliminates the inhomogeneous nature of the simple square array due to the periodic alignment of rows by the shift of the particles in every other row horizontally. The hexagonal array (PS3), shown

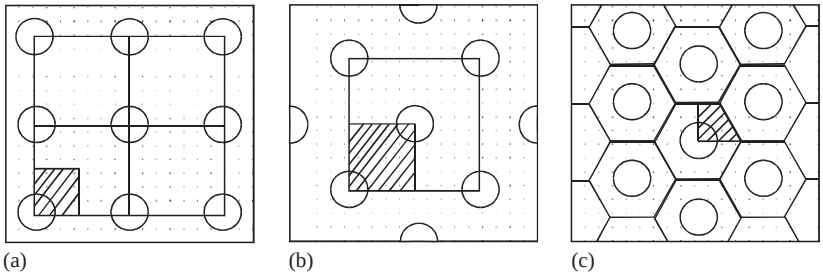


Fig. 1. Two-dimensional plane strain material idealizations: (a) simple square array (PS1); (b) staggered square array (PS2); and (c) stacked hexagonal array (PS3).

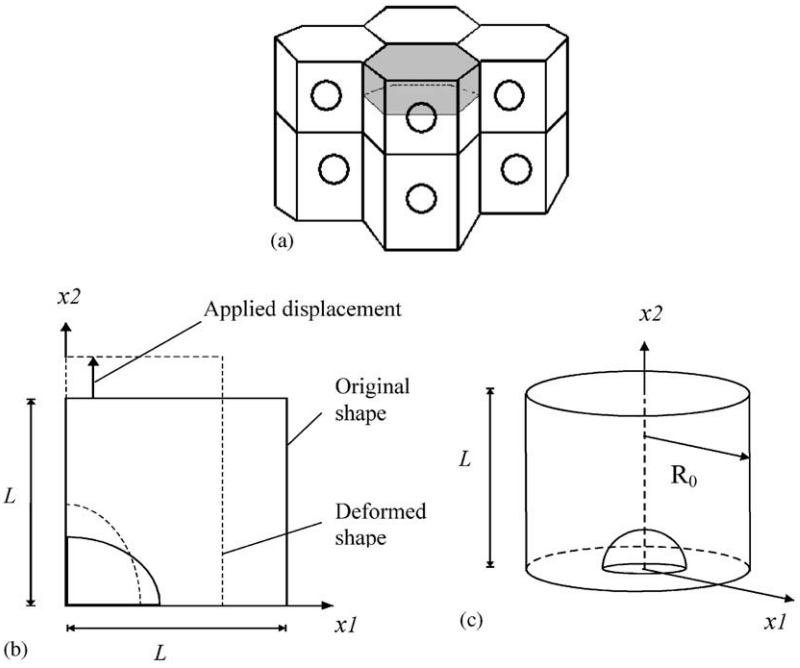


Fig. 2. The SHA model: (a) three-dimensional array of stacked hexagonal cylinders, each containing a spherical particle; (b) the deformed and undeformed shape of the RVE under axial loading; and (c) the SHA axisymmetric RVE cell.

in Fig. 1c, has also been used by some researchers, and shown to have accuracy similar to the staggered square array model.

Axisymmetric idealizations have been widely used and reported to accurately capture the real material behavior. It is reported by some authors (Socrate and Boyce [13]) that it provides a better representation of the morphology of real materials and captures the real material behavior more accurately, especially at high volume fractions of the harder phase. The most common axisymmetric model, the SHA RVE shown in Fig. 2 has been comprehensively used for different materials. This model is conceptually the axisymmetric analog of the idealization shown in Fig. 1a. A more recent

axisymmetric model developed by Socrate and Boyce [13], the body centered cubic (V-BCC), which differs from the SHA model in only the boundary condition with neighboring cells accounting for the interaction of adjacent cells, has also been employed by several researchers.

### 2.2. The constitutive behavior of each material phase

The behavior of each steel phase can be determined by tests on steels consisting of a single phase. This is achievable by heating the steel to the required temperature and then cooling at controlled rates using the time–temperature transformation (TTT) diagram to get the desired phase. The single-phase steels can then be tested in tension or compression to obtain the characteristic behavior of a specific phase. The constitutive behaviors of Bainite, Martensite, Pearlite and approximated behavior of Ferrite have been reported in the literature [18,20]. In the micromechanical model, the constitutive behavior of the constituents will only be required to investigate the aggregate behavior, which is thus far achievable. The interaction of phases (interface boundaries) will be ignored, as it is considerably small, on the order of few atomic sizes, compared to the phases being modeled.

Each phase is considered to be an elastic–plastic solid and it is assumed that the strain 'rate' can be additively decomposed into elastic and plastic components

$$\dot{\varepsilon}_{ij} = \dot{\varepsilon}^e_{ij} + \dot{\varepsilon}^p_{ij}, \tag{1}$$

where the elastic component is described by Hooke's law. The plastic strain rate is given as

$$\begin{aligned} \dot{\varepsilon}^p_{ij} &= 0, \qquad f < 0, \\ \dot{\varepsilon}^p_{ij} &= \frac{3}{2}\frac{\dot{\varepsilon}^p}{\sigma}\sigma'_{ij}, \quad f = 0, \end{aligned} \tag{2}$$

where the deviatoric stresses $\sigma'_{ij} = \sigma_{ij} - 1/3\sigma_{kk}$ and the equivalent stress, $\sigma$, and the equivalent strain rate, $\dot{\varepsilon}^p$, are defined as

$$\begin{aligned} \sigma &= \sqrt{\frac{3}{2}\sigma'_{ij}\sigma'_{ij}}, \\ \dot{\varepsilon}^p &= \sqrt{\frac{2}{3}\dot{\varepsilon}^p_{ij}\dot{\varepsilon}^p_{ij}}. \end{aligned} \tag{3}$$

The von Mises yield condition is assumed:

$$f = \sigma - \bar{\sigma}, \tag{4}$$

where $\bar{\sigma}$ is a function of the equivalent plastic strain and is taken to describe the isotropic hardening.

The hardening behavior of the two phases is taken from the experimental results obtained by Davies [21] and expressed by the following:

$$\begin{aligned} \bar{\sigma}_f &= K_f(\varepsilon_0 + \varepsilon^p_f)^{n_f}, \\ \bar{\sigma}_m &= K_m(\varepsilon_0 + \varepsilon^p_m)^{n_m}, \end{aligned} \tag{5}$$

where the subscripts $f$ and $m$ denote Ferrite and Martensite, respectively, and $\varepsilon_0$ is taken to be equal to 0.002 in this work, $K_m$ and $K_f$ are taken to be 2409 and 597 MPa, respectively and $n_m$ and $n_f$ are 0.07 and 0.31, respectively. The stress vs. plastic strain for each phase is shown in Fig. 3.

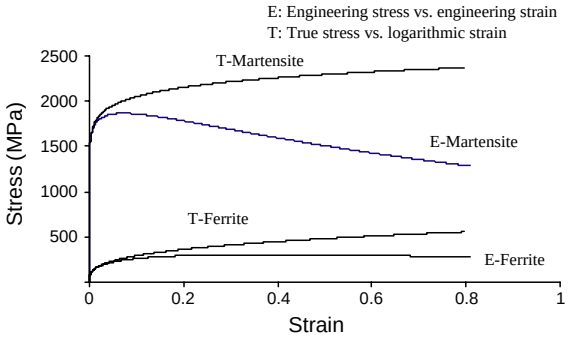


Fig. 3. Behavior of the Martensite and Ferrite phases shown as true stress vs. true strain and engineering stress vs. engineering strain for uniaxial tensile stress conditions.

To better illustrate the difference in uniform elongation between the two phases, the behavior under uniaxial tension stress is considered. Under these conditions, the equivalent stress reduces to the true uniaxial stress, $\sigma_{true}$, and the equivalent plastic strain is equal to the plastic strain along the direction of loading or true strain, $\varepsilon_{true}$. The corresponding engineering quantities are related to the true quantities as follows:

$$\varepsilon_{eng} = \exp(\varepsilon_{true}) - 1,$$
$$\sigma_{eng} = \sigma_{true}/(1 + \varepsilon_{eng}). \tag{6}$$

The engineering stress vs. engineering strain response for uniaxial tension loading is also shown in Fig. 3, where the difference in uniform strain (strain at maximum engineering stress) for the two phases is quite apparent. [1]

### 2.3. Homogenization method

The macroscopic stress components are computed as the volume average of the microscopic components according to the following equations:

$$S_{ij} = \frac{1}{V}\int_V \sigma_{ij}\,\mathrm{d}V, \tag{7}$$

$$E_{ij} = \frac{1}{V}\int_V \varepsilon_{ij}\,\mathrm{d}V, \tag{8}$$

where $S_{ij}$ and $E_{ij}$ are the macroscopic average component of stresses and strains over the microscopic volume of the micromechanical model. The macromechanical behavior of the aggregate is, therefore, approximated by the volume average of the micromechanical behavior. The question of how this averaging process is performed has an obvious effect on the accuracy of the aggregate constitutive model.

[1] It should be noted that no fracture criteria has been employed so the response shown cannot predict the limiting strain value of the phase under tensile loading.

## 3. Rule of mixtures

The microstructures that are obtained in steels from austenitic transformation comprise a widely dispersed range of mechanical properties. To estimate the mechanical properties of such materials, empirical equations describing the UTS and the 0.2% offset yield strength are often considered for single-phase materials [22,23]. For aggregates consisting of two or more phases, homogenization techniques, the most common of which known as the rule of mixtures are also commonly employed. The simplest of these assume either uniform strain, known as the Voigt estimate, or uniform stress, which is known as the Reuss estimate. The two estimates have been shown by Hill [24] to be upper and lower bounds, respectively. Using Eq. (5), the Voigt and Reuss bounds can be written as

$$\bar{\sigma}_c = V_m K_m (\varepsilon_0 + \varepsilon_m^p)^{n_m} + (1 - V_m) K_f (\varepsilon_0 + \varepsilon_f^p)^{n_f},$$

$$\varepsilon_c^p + \varepsilon_0 = V_m \left(\frac{\bar{\sigma}_m}{K_m}\right)^{1/n_m} + (1 - V_m) \left(\frac{\bar{\sigma}_f}{K_f}\right)^{1/nf}, \tag{9}$$

where the subscript '$c$' denotes the aggregate. As shown in Fig. 4, for low Martensite volume fractions the two bounds are relatively close, but at higher volume fractions the discrepancy is quite large. A modified form of the rule of mixtures was proposed by Bourell and Rizk [20]. The Ferrite part contains a term, which accounts for the influence of the Austenite–Martensite-induced transformation strain on the Ferrite matrix. This equation was also used to investigate the upper and lower bound of the stress vs. strain trend, as was done in Fig. 4. The results obtained using the modified rule of mixtures with the prestrain induced in the Ferrite matrix by the Austenite–Martensite transformation at different volume fractions of the harder phase show that the difference between the ordinary and modified rule of mixtures to be negligible at low $V_m$ and about 1–2% at high $V_m$. The large discrepancy in the upper and lower bound in either case demonstrates the need to use methods other than the simple rule of mixtures for predicting the aggregate response.

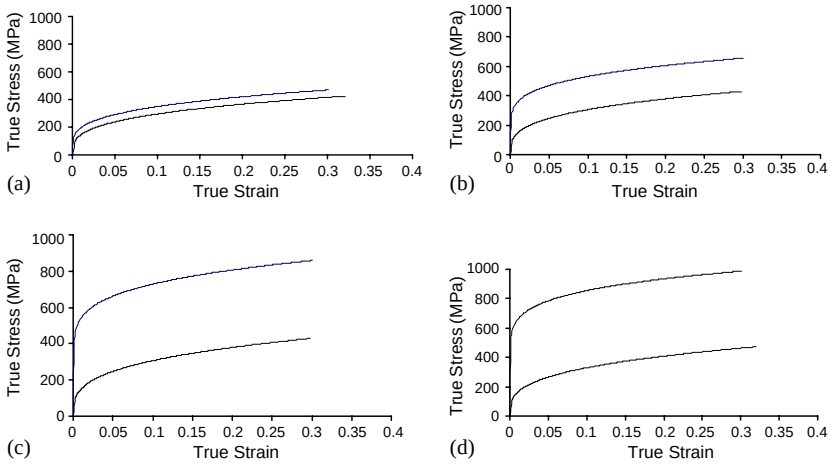


Fig. 4. Upper and lower bound predicted by ROM for several volume fractions, $V_m$: (a) 3.2%; (b) 13.6%; (c) 24.8%; and (d) 32%.

Different straining models based on rule of mixtures have been used in the past by various authors in analyzing the strength of DP steels. Two main assumptions were made, one assumes the material as a mixture of two ductile phases deforming at the same ratio, also called isostrain models. On the other hand, the second assumption made by some workers followed Ashby's theory of particle strengthening [25]. Others like Speich and Miller [26] and Szewczyk and Gurland [27] considered the difference between the strain in the Martensite and Ferrite but held the strain ratio constant throughout the entire tensile process. A comprehensive review of the above is given by Szewczyk and Gurland [27] and Korzekwa et al. [28]. Elastic–plastic behavior of two-phase polycrystalline materials have also been predicted by using the Mori–Tanaka [29] method, which is used as the basis for many continuum analytical models [30–32].

Korzekwa et al. [28] presented a detailed evaluation of the methods such as the rule of mixtures, isostrain assumption, strain partitioning models (also called continuum models) and the isostress models. They asserted that although most of the treatments predict the increase in strength and decrease in ductility that accompany an increase in $V_m$ reasonably well, some of the correlations may be fortuitous as the basic assumption used to model the strain distribution between the Ferrite and Martensite are inconsistent with experimental microscopic observations they presented. Ostrom [33] in a study of the analytical models concluded that without knowledge of how stress and strain develop in the two phases during deformation, no conclusive results could be reached and thus the models based on rule of mixtures are not reliable. In addition, the traditional simulations of the deformation and fracture of solids by application of continuum mechanics and averaged macroparameters or homogenization methods are not sufficient for developing a predictive theory of deformed solids. Internal microstructure evolution should also be considered as they affect the mechanical properties of materials substantially. Local values of the elastic–plastic parameters at the microlevel differ widely from the averaged macrodata, a fact widely validated and accepted. The computational micromechanical methods provide these local data. In this work the micromechanical modeling of cells is used to understand the mechanics and mechanism of deformation in DP steels.

## 4. Finite element modeling

Finite element analysis, using several different micromechanical models, has been used to carry out the homogenization procedure. The analyses considered were limited to 2D, plane strain and axisymmetric cases to keep computational time reasonable. The analysis was performed using the commercial code ABAQUS. Each phase, namely Martensite and Ferrite, is considered to be an elastic–plastic solid as described by Eqs. (1)–(5), with $E = 200$ GPa and $\nu = 0.3$.

Two plane strain idealizations, namely the PS1 and PS2, are considered in this work. The PS2 idealization is developed in order to better capture the interaction between the neighboring hard particles, as previously discussed. The PS3 idealization has been reported by Socrate and Boyce [13] to display very similar results as the PS2 and thus has not been considered. Four-noded, linear, quadrilateral (axisymmetric and plane strain) elements were used. The same mesh is used for the SHA and PS1 idealizations, differing only in element type. Due to symmetry, only the shaded area of Fig. 1 is modeled.

Referring to Fig. 5, the volume fraction, $V_m$, is computed as $\pi a^2/4L^2$ and $2/3a^3/L^3$ for the plane strain and axisymmetric cases, respectively. Referring to the same figure, symmetry boundary

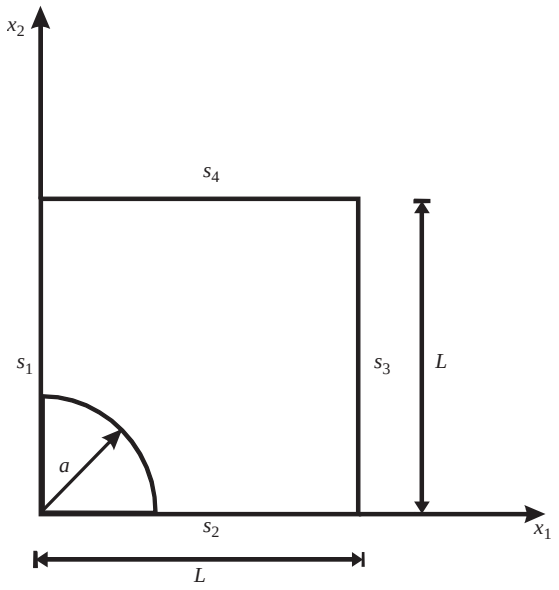


Fig. 5. Dimensions of the micromechanical model.

conditions are used for sides S1 and S2, while side S3 has a uniform displacement in the $x_1$ direction and side S4 has uniform displacement in the $x_2$ direction. Cases for specified displacement in the $x_2$ direction on side S4 as well as specified normal traction have both been considered. The aggregate strains are computed as

$$E_{11} = \ln(u_1(L, x_2)/L),$$
$$E_{22} = \ln(u_2(x_1, L)/L). \tag{10}$$

The engineering normal stress in the $x_2$ direction is computed from the resultant force divided by the original area, from which using Eq. (6), the Cauchy stress component is computed. For the SHA micromodels the state of stress is uniaxial, such that the $S_{22}$ and $E_{22}$ components of stress and strain are equal to the corresponding equivalent quantities. For the plane strain case ($E_{33} = 0$), $S_{33}$ is well approximated by the intermediate value of the other normal stresses ($S_{33} = (S_{11} + S_{22})/2$) after a plastic strain a few times the strain at yield [34]. Since $S_{11} = 0$, $S_{33}$ is taken to be $S_{22}/2$ and the equivalent stress and strain are computed from Eq. (3).

Each mesh has also been subjected to both prescribed traction and displacement boundary conditions along side S4 (see Fig. 5). For a properly developed RVE, the homogenization procedure should yield the same equivalent stress vs. equivalent strain as described by Hill [24]. The comparison for PS1 for a $V_m$ of 11.8% is shown in Fig. 6. Similar results were obtained for the other two models.

The predicted response for the aggregate is computed for each case for varying Martensite volume fractions as shown in Fig. 7. The engineering stress vs. engineering strain response is chosen to present the results so that the difference in uniform strain (strain at maximum engineering stress) can be seen clearly as this would not be possible to observe in the true stress vs. logarithmic strain.

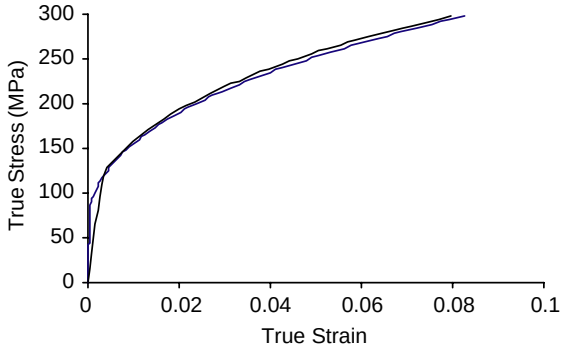


Fig. 6. Comparison of behavior predicted for the aggregate material using traction and displacement boundary conditions on side S4 for the PS1 model and $V_m = 11.8\%$.

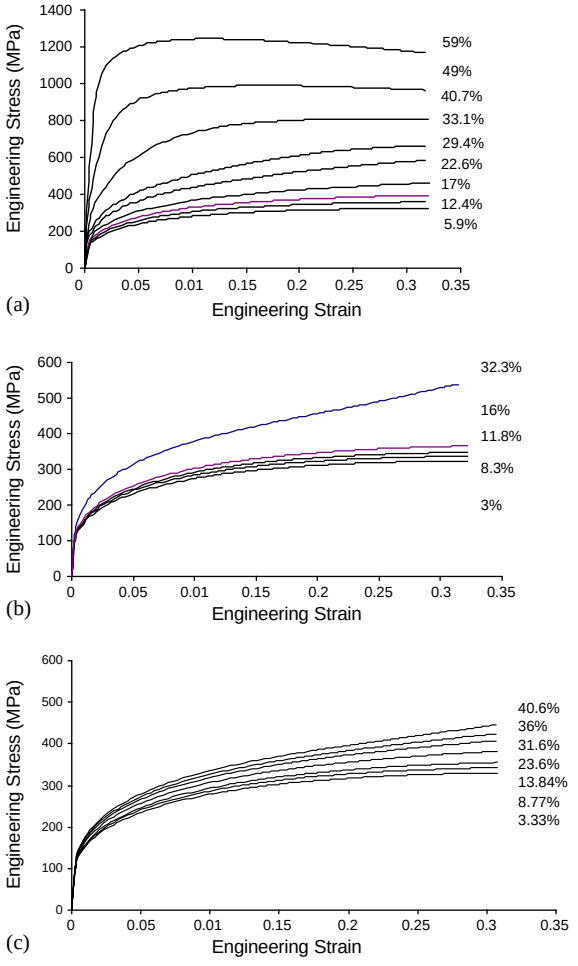


Fig. 7. Computed engineering stress vs. engineering strain under uniaxial tensile stress conditions for varying $V_m$: (a) SHA model; (b) plane strain (PS1) model; and (c) plane strain (PS2) model.

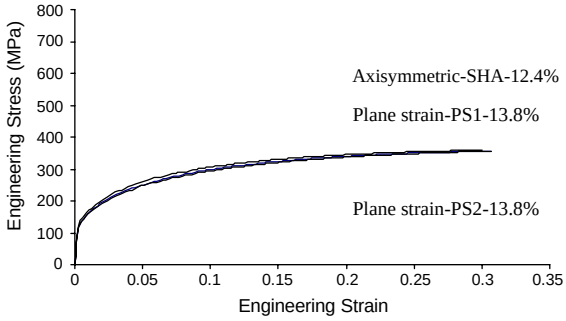


Fig. 8. Comparison of computed behavior using different models for low Martensite volume fraction.

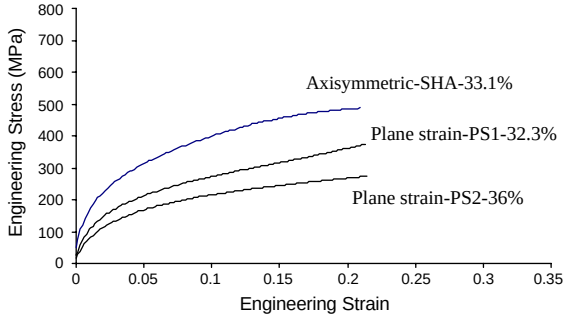


Fig. 9. Comparison of computed behavior using different models for high Martensite volume fraction.

As shown in Fig. 8, the response given for each model is quite similar at low volume fractions. However, significant differences become apparent for volume fractions above approximately 23%. Fig. 9 shows the results for the different models at an approximate volume fraction of 32–36%. The response for the axisymmetric SHA model is quite similar and consistent with experimentally observed behavior, i.e. engineering stress increases up to a maximum, which occurs at the onset of instability. The plane strain models appear to overpredict strain hardening, which unrealistically suppresses the localization. This can also be seen in Figs. 7b and c, where increasing $V_m$ results in increasing hardening, which is contradictory to what is observed experimentally [4,5,7,8].

The evolution of equivalent plastic strain for the axisymmetric, PS1 and PS2 idealizations are shown in Fig. 10, corresponding to nominal strains of 10%, 20% and 30%. All three models show the heterogeneous distribution of strain, which agrees with experimental observations of Shen et al. [8] and Rashid and Cprek [2]. However, only the axisymmetric SHA model shows plastic strain extending into the Martensite. In both plane strain models the Martensite remains elastic. Although the amount of plastic strain in the Martensite is quite small ($< 8\%$), the effect on the overall material response is significant. This is demonstrated quite clearly in Fig. 11, which compares the response in the axisymmetric case treating the Martensite as an elastic solid to that when the Martensite is considered an elastic–plastic solid. Treating the material as an elastic solid results in a response, which is, quite similar to that observed in the plane strain models, and contrary to experimental observations. The plastic deformation of the Martensite is, therefore, judged to be quite important

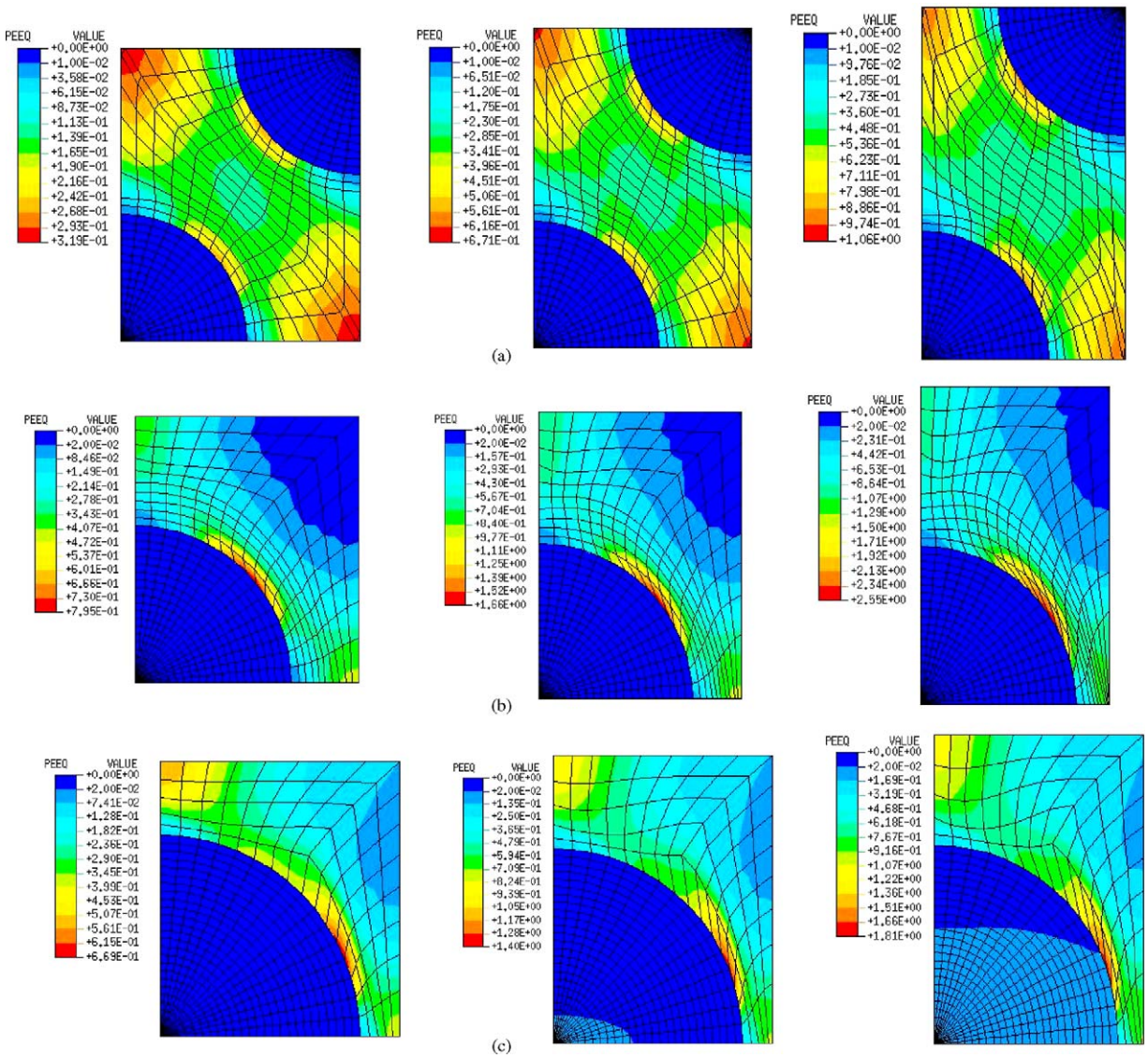


Fig. 10. Contours of equivalent plastic strain for nominal strains of 10%, 20%, and 30%: (a) plane strain (PS2) model; (b) plane strain (PS1) model; and (c) the SHA axisymmetric model.

and must necessarily be captured by an appropriate micromechanical model. In the case of the constituent behavior considered here, this only occurs for the axisymmetric model.

## 5. Conclusion

Of the cases considered, only the axisymmetric SHA model displays the trend of increase in the engineering stress and the reduction of the onset of strain localization with increasing $V_m$. In both

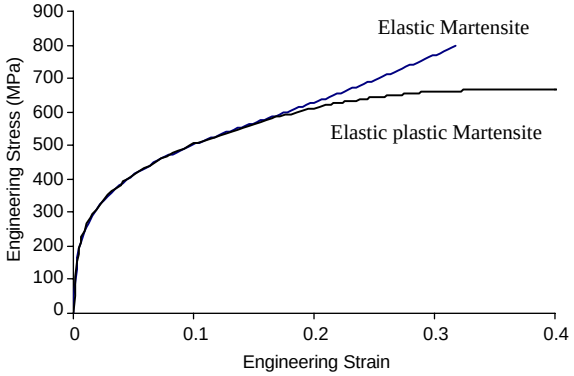


Fig. 11. Predicted behavior using SHA axisymmetric model with $V_m = 29.4\%$ treating Martensite as an elastic and an elastic–plastic solid.

PS1 and PS2 cases, the strain hardening in the material was overpredicted which unrealistically suppressed localization as shown in Figs. 7(b,c).

The above phenomenon is believed to occur for several reasons. The most significant of which is attributed to the deformation stages, which take place in the Martensite particles and the Ferrite matrix. As mentioned earlier, Shen et al. [8] and Rashid and Cprek [2] have shown experimentally, using scanning electron microscopic micrographs, that the Martensite particles deform after the Ferrite matrix is excessively deformed. Shen et al. [8] have also shown using a scanning electron microscopy equipped with a straining stage that at low $V_m$ only the Ferrite matrix deforms with no measurable strain occurring in the Martensite particles. Very small strains in the peripheral areas of Martensite islands were reported using an interferential microscope. At high $V_m$ they have shown that shearing of the interface between Martensite and Ferrite occurs extending the strains into the Martensite islands.

All the models considered have similar stress–strain trends at low $V_m$ as depicted in Fig. 8. The Martensite particles undergo no measurable strain, which is in agreement with experimental observation by Shen et al. [8]. At high $V_m$, the Martensite particles in PS1 and PS2 models behave elastically while it plastically deforms in the axisymmetric SHA case. Although, the plastic deformation that takes place in the Martensite particles is small, it is believed to be an important phenomenon, which alters the mechanics of deformation of the aggregate significantly as shown in Fig. 11. The inability of plane strain models to show any plastic deformation in the Martensite particles is believed to be the main reason behind the suppression of the localization behavior they display. In the plane strain idealization, the Martensite particles are geometrically assumed to be long cylinders in a Ferrite matrix, rather than a spherical particle in a cylindrical matrix. As a result, for the same volume fraction, the area fraction of Martensite is larger in the axisymmetric model, causing yield to occur at lower strains, which more closely resembles the actual material response.

Shen et al. [8] reported the extent to which the Martensite and Ferrite particles deform and show that, in addition to strain being inhomogeneous in both the Ferrite and the Martensite, strains in both increase linearly with increasing the macroscopic strain of the specimen. They have also reported that the Martensite plastic deformation is negligible at nominal strain levels of about 10% and in the range of 5–10% at 30% nominal strain of the specimen, which agrees well with results

observed in the axisymmetric SHA model. It is worthwhile mentioning that Shen et al. [8] reported Martensite deformation levels for various combinations of $V_m$ and %C in the steel. Increasing the $V_m$ with constant %C in the steel would cause dilution of the carbon in the Martensite particles, which reduces its strength, but this is reported to be significant only in volume fractions above 30%. Dilution effect in the levels of $V_m$ reported by Shen et al. [8] are negligible as the plastic deformation of the Martensite particles are reported to be very close in all the cases.

In this work, a micromechanical model for the DP steels consisting of Martensite particles dispersed in a matrix of Ferrite has been developed. The axisymmetric idealization proved to capture the material behavior of this material both in terms of general stress–strain trend and in terms of deformation fields in both constituents of the aggregate. The axisymmetric model is shown to capture the mechanism of deformation of DP steels observed and reported in the literature, of displaying the three phases of deformation as mentioned in the material background. The model succeeded in capturing the trend of increase in strength and uniform strain with increasing volume fraction of Martensite to a certain value and then increasing strength and decrease of uniform strain with further increase in volume fraction. This model will prove valuable for determining optimum $V_m$ for DP steels while minimizing the amount of required experimental work. In addition, it provides a unique tool for understanding the mechanics and mechanisms of deformation taking place in such materials which can be used in developing a predictive theory of deformed solids for both ductile failure or failure under fatigue loading.

## Acknowledgements

The authors wish to acknowledge the support of the AUTO 21 Network of Centers of Excellence and the Natural Sciences and Engineering Research Council of Canada. The first author wishes to acknowledge the financial support of University of Bahrain.

## References

[1] Rashid MS. GM 980X-A unique high strength sheet steel with superior formability. SAE preprint Detroit 1976; paper number 760206, p. 23–7.
[2] Rashid MS, Cprek ER. Relationship between microstructure and formability in two high-strength low-alloy steels. In: Niemeier BA, Schmieder AK, Newby JR, editors. Formability topics—metallic materials, ASTM STP 647. Philadelphia, PA: American Society for Testing and Materials; 1978. p. 174–90.
[3] Jiang Z, Guan Z, Lian J. The relationship between ductility and material parameters for dual phase steel. Journal of Materials Science 1993;28:1814–8.
[4] Bag A, Ray KK, Dwarakadasa ES. Influence of Martensite content and morphology on tensile and impact properties of high-Martensite dual-phase steels. Metallurgical and Materials Transactions 1999;30(A):1193–202.
[5] Tomita Y. Effect of morphology of second-phase Martensite on tensile properties of Fe-0.1C dual phase steels. Journal of Materials Science 1990;25:5179–84.
[6] Byun TS, Kim IS. Tensile properties and inhomogeneous deformation of Ferrite–Martensite dual-phase steels. Journal of Materials Science 1993;28:2923–32.
[7] Tomota Y. Effects of morphology and strength of Martensite on cyclic deformation behavior in dual-phase steels. Materials Science and Technology 1987;3:415–21.
[8] Shen HP, Lei TC, Liu JZ. Microscopic deformation behavior of Martensitic–Ferritic dual-phase steels. Materials Science and Technology 1986;2:28–33.
[9] McClintock FA. A criteria for ductile fracture by growth of holes. Journal of Applied Mechanics 1968;35:363–71.
[10] Rice JR, Tracey DM. On the ductile enlargement of voids in triaxial stress fields. Journal of the Mechanics and Physics of Solids 1969;17:201–17.

[11] Gurson AL. Continuum theory of ductile rupture by void nucleation and growth: Part I—yield criteria and flow rules for porous ductile media. Journal of Engineering Materials and Technology 1977;99:2–15.
[12] Tvergaard V. Influence of voids on shear band instabilities under plane strain conditions. International Journal of Fracture Mechanics 1981;17:389–407.
[13] Socrate S, Boyce MC. Micromechanics of toughened polycarbonate. Journal of the Mechanics and Physics of Solids 2000;48:233–73.
[14] Huang Y, Kinloch AJ. Modeling of the toughening mechanisms in the rubber-modified epoxy polymers: Part I—finite element analysis studies. Journal of Materials Science 1992;27:2753–62.
[15] Socrate S, Boyce MC, Lazzeri A. A micro mechanical model for multiple crazing in high impact polystyrene. Mechanics of Materials 2001;33:155–75.
[16] Tzika PA, Boyce MC, Parks DM. Micromechanics of deformation in particle toughened polyamides. Journal of the Mechanics and Physics of Solids 2000;48:1893–929.
[17] Tvergaard V. Effect of void size difference on growth and cavitation instabilities. Journal of the Mechanics and Physics of Solids 1996;44:1237–53.
[18] Ishikawa N, Parks DM, Socrate S, Kurihara M. Micromechanical modeling of Ferrite–Pearlite using finite element unit cell models. Iron and Steel Institute of Japan International 2000;40(11):1170–9.
[19] Huper T, Endo S, Ishikawa N, Osawa K. Effect of volume fraction of constituent phases on the stress relationship of dual phase steel. Iron and Steel Institute of Japan International 1999;39:288–94.
[20] Bourell DL, Rizk A. Influence of Martensite transformation strain on the ductility of dual phase steels. Acta Metallurgica 1983;31:609–17.
[21] Davies RG. The mechanical properties of zero-carbon Ferrite-plus-Martensite structures. Metallurgical Transactions 1978;9(A):451–5.
[22] Pickering FB. Physical metallurgy and design of steels. London: Applied Science Publishers LTD; 1978.
[23] Gladman T. The physical metallurgy of microalloyed steels. London: The Institute of Materials; 1997.
[24] Hill R. Elastic properties of reinforced solids: some theoretical principles. Journal of the Mechanics and Physics of Solids 1963;11:357–72.
[25] Balliger NK, Gladman T. Work hardening of dual-phase steels. Metal Science 1981;15(3):95–108.
[26] Speich GR, Miller RL. Mechanical properties of Ferrite–Martensite steels. In: Kot RA, Morris JW, editors. Structure and properties of dual-phase steels. New York: TMS-AIME; 1979. p. 145–82.
[27] Szewczyk AF, Gurland J. A study of the deformation and fracture of a dual-phase steel. Metallurgical Transactions 1981;13(A):1821–6.
[28] Korzekwa DA, Lawson RD, Matlock DK, Krauss G. A consideration of models describing the strength and ductility of dual-phase steels. Scripta Metallurgica 1980;14:1023–8.
[29] Mori T, Tanaka K. Average stress in matrix and average elastic energy of materials with misfitting inclusions. Acta Metallurgica 1973;21:571–4.
[30] Weng GJ. The overall elastoplastic stress–strain relations of dual-phase metals. The Journal of the Mechanics and Physics of Solids 1990;38(3):419–41.
[31] Tomota Y, Kuroki K, Mori T, Tamura I. Tensile deformation of two-phase alloys: flow curves of $\alpha$–$\gamma$ Fe–Cr–Ni alloys. Materials Science and Engineering 1976;24:85–94.
[32] Rudiono, Tomota Y. Application of the secant method to prediction of flow curves in multi-microstructure steels. Acta Metallurgica 1997;45(5):1923–9.
[33] Ostrom P. Deformation models for two-phase materials. Metallurgical Transactions 1981;12(A):355–7.
[34] Hill R. The mathematical theory of plasticity. New York: Oxford University Press; 1950.